Drastically enhanced H_{2} flux through asymmetric quantum Pd films

Guangfen Wu, Wenguang Zhu, Jinlan Wang, and Zhenyu Zhang

Drastically Enhanced H$_2$ Flux through Asymmetric Quantum Pd Films

Guangfen Wu[1,2], Wenguang Zhu[2,†], Jinlan Wang[1,*], and Zhenyu Zhang[3,4]

[1]*Department of Physics, Southeast University, Nanjing, 211189, China*

[2]*Department of Physics, University of Tennessee, Knoxville, Tennessee, 37996, USA*

[3]*ICQD/HFNL, University of Science and Technology of China, Hefei, Anhui, 230026, China*

[4]*School of Applied Science and Engineering, Harvard University, Cambridge, MA 02138, USA*

ABSTRACT: It has been established recently that the quantum mechanically confined motion of conduction electrons within ultrathin metal films can strongly modify the various atomic rate processes and chemical reactivity on top of the films with thickness-dependent stability. In this work, we investigate theoretically how such quantum size effects (QSE) can alter the energetics and kinetics as gaseous hydrogen molecules adsorb dissociatively on one side of an ultrathin Pd membrane serving as a model separating system, and desorb associatively from the other side. We first establish that these quantum Pd films possess extra (or magic) stability at certain film thicknesses, and demonstrate that the H$_2$ flux through such quantum films can be tuned significantly by the QSE-induced variations in the key molecular/atomic rate processes. Furthermore, when the permeate side of the films is coated with a layer of less H-reactive Cu or Ag element, the depth of the H chemisorption well is lowered substantially without introducing other larger barriers, which in turn can enhance the H$_2$ flux by several orders of magnitude around 500 K. These findings of fundamental nature may prove to be inspirational in future design of ideal membrane-based devices with maximal hydrogen permeability and low cost.

PACS numbers: 73.21.Fg , 66.30.–h, 82.20.Kh, 82.30.Rs

I. Introduction

Quantum mechanically confined motion of conduction electrons within ultrathin metal films or related metal nanostructures gives rise to discrete energy levels or subbands, which in turn may render these nanomaterials new properties different from their bulk counterparts.[1-8] Indeed, such quantum size effects (QSE) play a determinant role in the formation and stability of the metal films, leading to self-assembled growth of atomically flat films with highly selective thicknesses, a phenomenon dubbed "electronic growth" or "quantum growth".[2] Extensive efforts have been devoted to exploiting how such QSE can also strongly modify the various atomic rate processes and chemical reactivity on top of the ultrathin metal films with thickness-dependent stability.[9-17] For example, bi-layer oscillations in the growth morphology of Pb/Si (111)[18] and thickness-dependent Fe island density on wedged Pb films[19] have been observed experimentally stemming from QSE modulated surface adatom mobility. Dramatic oscillations in the desorption temperature of CO on ultrathin Cu films as a function of film thickness have also been observed, which has been attributed to the existence of two dimensional quantum well subbands crossing the Fermi level.[9] Similarly, it has been demonstrated that the oxidation rate of ultrathin Mg(0001) films on W(110) oscillates as a function of the film thickness, and correlates well with the oscillatory decay lengths of the quantum well states;[10] especially, thickness variation of only one atomic layer has been shown to result in a change of factor 3 in the surface oxidation of quantum Pb films.[13]

In this work, we investigate a more complex and conceptually intriguing problem, namely, how QSE can alter the energetics and kinetics as gaseous hydrogen molecules transport through

an ultrathin metal film, with Pd-based membranes as prototypical systems. Purification of hydrogen using Pd-based films (usually with their thicknesses in the bulk-like regime) has been widely explored using both theoretical and experimental approaches, because of their high permeability, high selectivity, and chemical compatibility with many hydrocarbon-containing gases.[20-28] Nevertheless, the high cost of such thick films, lower-than-desirable permeability, and long-term stability still stand as major obstacles against large-scale applications.[29-31] Separately, a recent experimental advance has been achieved by Huang *et al.* in synthesizing atomically flat freestanding hexagonal palladium nanosheets that are only less than 10 atomic layers thick,[32] which may have a wide range of new application potentials. In particular, exploration of such Pd-based quantum films for hydrogen purification may not only offer insights into dramatically reducing the cost of Pd due to increased area/volume ratios, but such studies may also reveal extra tunability in the H-reactivity and overall permeability of the films.

Aside from invoking QSE for improved permeance, additional functionalization of the pure Pd quantum films may offer further enhancement. In particular, in this thin-film, surface-effect dominant regime, since the decomposition of H_2 on the feed side is almost a spontaneous process, we expect that coating of the permeate side with less H-reactive metal can significantly lower the desorption barrier, thus enhancing the H_2 flux. Interestingly, for a reverse purpose of hydrogen storage, previous studies showed that magnesium thin films capped with palladium layers on both sides can significantly increase the hydrogen pressure inside the films.[33] Moreover, earlier studies revealed that the recombination rate of H_2 on the surface of Cu is larger than that on Pd.[34,35] However, reduced H_2 fluxes was reported experimentally when a thin Cu layer (3-5 nm)

3

was coated on the permeate side of Pd membranes (of thicknesses ~100 μm).[36] These somewhat conflicting findings of hydrogen permeability involving much thicker Pd, Cu, and Cu-coated Pd films offer yet additional incentives to carry out a more systematic study of these systems, particularly in the ultra-thin, quantum regime based on first-principles approaches.

Here we explore the feasibility of using ultra-thin Pd quantum films as potential building blocks in developing membrane technologies with high H_2 permeability using a multi-scale approach combining first-principles calculations within density-functional theory (DFT) with rate equation simulations. We demonstrate that QSE can dramatically tune the H_2 flux through the ultrathin quantum films. More strikingly, functionalization of the Pd films (in the surface effect dominated thickness regime) with the coating of a less H-reactive Cu or Ag monolayer can dramatically reduce the rate-limiting barrier, thereby increasing the H_2 flux at ~500K by as high as respectively 5 or 4 orders of magnitude over the flux for symmetric pure Pd films.

II. Computational Methods

The DFT calculations were carried out using the Vienna *ab* initio simulation package (VASP)[37] with the projector augmented wave (PAW) method and the generalized gradient approximation (PBE-GGA)[38] for exchange correlation. The ''climbing image nudged elastic band'' method[39] was used for the calculation of energy barriers for the various kinetic processes. The Monkhorst-Pack scheme was adopted for the Brillouin zone sampling with a 24 × 24 × 1 and 3 × 3 × 1 k-point mesh for pristine Pd films and Pd films with H adsorption at 1/4 ML coverage, respectively. A supercell containing 1 × 1 and 4 × 4 primitive unit cells was used with

a vacuum region of 15 Å, large enough for the system to converge to a correct total energy. In these calculations, all the atoms in a slab were fully relaxed. The cutoff energy used for the plane-wave basis set was 260 eV and the structural relaxation was done when all the forces on the atoms were smaller than 0.01 eV/Å. The calculated Pd lattice constant of 3.95 Å is very close to the experimental value of 3.89 Å, validating the accuracy of this computational method.

III. Results

A. Stability of quantum films

We first study the stability of symmetric and metal (Ag, Cu) coated asymmetric freestanding Pd quantum films along the [111] direction up to 20 layers. For an asymmetric film with a total thickness of N ML, the Ag or Cu monolayer is coated on the permeate side of an (N-1)-ML Pd film; the most stable stacking is obtained by placing the coating layer with the same lattice sequence of the pure N-ML Pd film, and is denoted by (N-1)Pd1Ag and (N-1)Pd1Cu, respectively. The second differences of the surface energies ($\delta^2 E/\delta N^2 = E_{N+1} + E_{N-1} - 2E_N$, E_N being the total energy of an N-ML film)[8] for the NPd, (N-1)Pd1Ag, and (N-1)Pd1Cu films as a function of the total film thickness are displayed in Figure 1, with positive values indicating stable films. The stability of these films shows considerable variations due to QSE, with the 4 ML possessing particularly high stability, characterizing it as a magic thickness in all the three systems. We also observe stable films at 7 ML and 10 ML film thicknesses, and the existence of magic thicknesses in this thickness regime is consistent with experimental observations.[32]
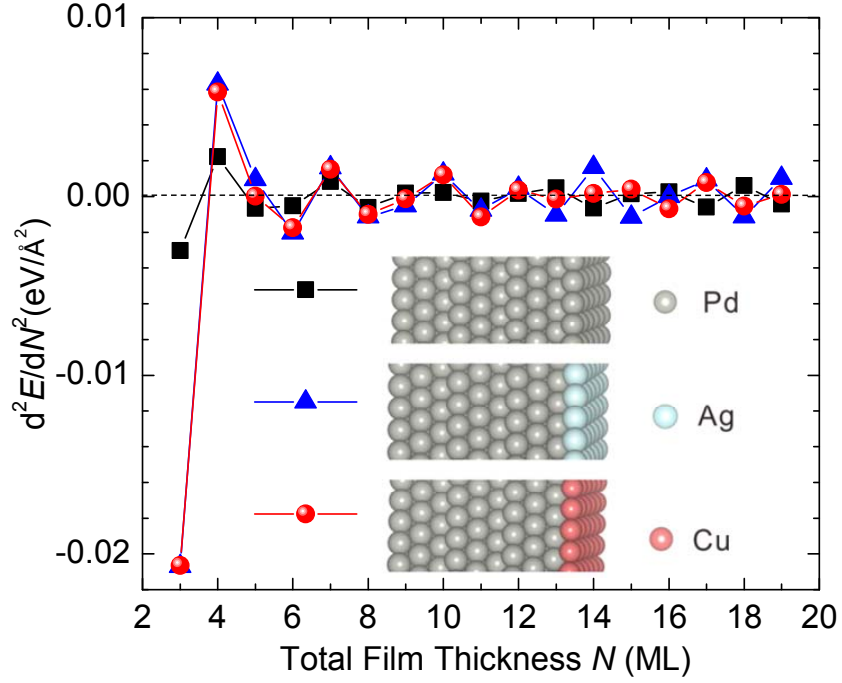
Figure 1. Second differences of the surface energies for NPd, $(N$-1)Pd1Ag, and $(N$-1)Pd1Cu films. The black dashed line is given as guide to the eye.

B. Quantum size effects on the energetics and kinetics of hydrogen interaction with pure Pd films

The permeation of H_2 through a metal film usually involves the following elemental molecular/atomic rate processes successively from the high pressure to low pressure side:[23] (1) H_2 decomposition; (2) surface-subsurface diffusion of H atoms; (3) subsurface-bulk diffusion of H atoms; (4) bulk diffusion of H atoms; (5) bulk-subsurface diffusion of H atoms; (6) subsurface-surface diffusion of H atoms; and, finally, (7) recombinative desorption of H_2. For thin Pd films, the surface effect, namely, the various atomic rate processes at or near the surfaces, dominates the whole permeation cycle. Therefore, we now investigate the thickness-dependent

surface H-reactivity of symmetric quantum Pd films. We place 1/4 ML of atomic H on all possible surface or subsurface sites and find the following trends: A surface *fcc*-site is energetically slightly favored over a surface *hcp*-site by less than 0.01 eV; at the subsurface depth level, H prefers to adsorb at an octahedral site rather than a tetrahedral site by about 0.1-0.2 eV; H adsorption on a surface *fcc* site is ~0.35 eV more stable than that on a subsurface octahedral site; the thicknesses-dependent variations of H binding energies near the surface due to the QSE are less than 0.04 eV. As surface-subsurface diffusion is an important step for H_2 separation,[40] we also examine the influence of the Pd film thickness on the kinetics of this process with selected thicknesses of 4, 6, 7, and 13 ML, and find that the barriers are about ~0.4 eV with variations less than 0.05 eV for different thicknesses.

C. Energy landscape of H permeation through 4-ML symmetric and asymmetric films

As the 4-ML films possess extremely high stability and the H penetration from surface to subsurface is easier, we next look into the thermodynamic and kinetic aspects of hydrogen permeation through 4Pd, 3Pd1Ag, and 3Pd1Cu films. The simplified energy landscapes of H_2 penetrating through these films are displayed in Figure 2, in which we incorporate the horizontal in-plane diffusion of H. The decomposition barrier of H_2 on the surface of pure Pd is negligible (0.04 eV), while the barrier for the reverse process (desorption) is high (1.36 eV), in line with the deep chemisorption well of H on the surface (Figure 2a). The second largest barrier, corresponding to surface-subsurface diffusion, is 0.4 eV, much smaller than the desorption one.

To reduce the well depth of H adsorption on the permeate side, we replace 1 ML of surface

Pd with 1 ML of Cu or Ag, known to have weaker bonding to H than Pd. As seen from Figure 2, the binding of H on the permeate side surface of 4Pd and 3Pd1Cu is 0.68 and 0.34 eV more favorable than free H_2 respectively, and becomes unfavorable by 0.25 eV for 3Pd1Ag. Furthermore, on the permeate side, the hydrogen adsorption on the surface is 0.34 and 0.29 eV more stable than that on the subsurface for 4Pd and 3Pd1Cu, respectively, and is 0.24 eV less stable for 3Pd1Ag. Consequently, the H_2 desorption from the permeate side of the 3Pd1Ag film is a spontaneous process. Without considering the subsurface-surface diffusion, we might conclude that the 3Pd1Ag film were a perfect system for hydrogen permeation. However, a large barrier of 0.95 eV appears against H penetration from the subsurface site to the Ag surface in the 3Pd1Ag system, a value not too much lower than the H_2 desorption barrier of 1.36 eV from a Pd surface. In contrast, on the permeate side of the 3Pd1Cu film, the H_2 desorption barrier is lowered to 0.79 eV, and the corresponding decomposition barrier is raised to 0.25 eV. Furthermore, the barrier against subsurface-to-surface diffusion of H increases only slightly to 0.1 eV from 0.04 eV in the pure Pd case. Therefore, desorption from the permeate side is the rate-limiting process for hydrogen permeation through the 4Pd and 3Pd1Cu films, while for 3Pd1Ag the rate-limiting process is the subsurface-to-surface diffusion. The reduced desorption barriers are consistent with the relatively weak binding between atomic H and Ag or Cu and can be understood by the d-hybridization picture that the positions of the d-band centers follow the order $E_d(Ag) < E_d(Cu) < E_d(Pd)$. [35,41,42]
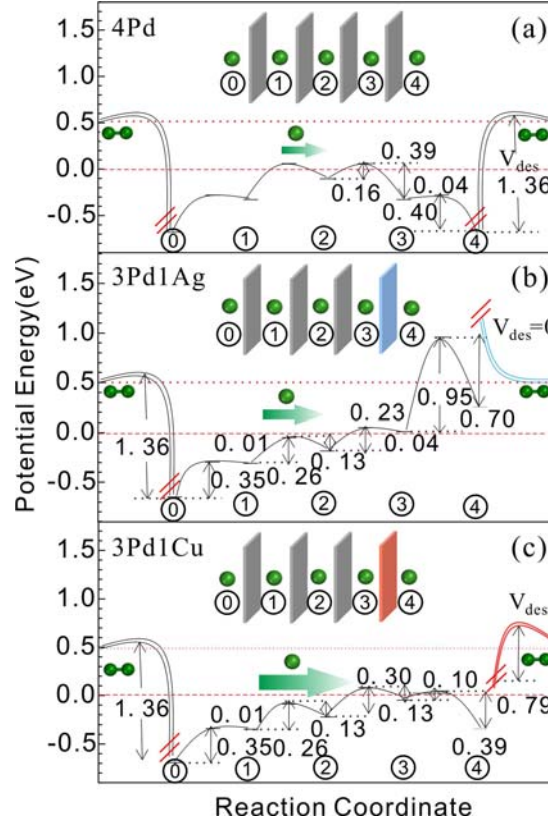
Figure 2. The energy landscapes of H$_2$ permeation through (a) 4Pd, (b) 3Pd1Ag, and (c) 3Pd1Cu. Single lines: energetics of atomic H transport through the films (the energy is scaled to that of a free hydrogen molecule H$_2$ far away from the surface); double lines: energetics of the H$_2$ decomposition and recombination processes. The curves are discontinuous because for the decomposition and recombination processes we use twice the values for atomic H transport. The red dashed lines indicate half of the energy level of a free H$_2$, and the red dotted lines are to guide the eye.

D. Rate equation model for deriving the H$_2$ flux

The quasi-steady state H$_2$ fluxes through the NPd, (N-1)Pd1Ag, and (N-1)Pd1Cu films with thicknesses ranging from 4 to 100 ML are estimated by analyzing the diffusion equation from a

9

microscopic view. A one-dimensional (1D) lattice model is applied without considering the H-H interaction (known as the tracer diffusion regime for dilute H concentrations[43,44]). For simplicity, we also assume that the feed side surface of a film is always fully occupied by atomic hydrogen, namely, the H/Pd ratio is 1.0. At time $t = 0$, the dimensionless hydrogen concentration on the feed side surface (c_0) equals 1.0, and that on other layers (c_i) is 0.0. This approximation is justified by the fact that saturated occupation of H will be rapidly established on the feed side surface even at moderate temperatures and under very low pressures, because of the deep chemisorptions well on the Pd surface. The *fcc* metal lattice is simplified into a 1D cubic lattice, and the permeation is described by a series of independent hydrogen jumps between adjacent sites in the 1D lattice. Moreover, since the associative desorption barrier of H_2 from the Pd surface is very large (1.36 eV) and the hydrogen partial pressure in the gas phase is high on the feed side, we ignore molecular desorption from the feed side surface. Given the ultra high vacuum conditions on the permeate side, the dissociative adsorption process of H_2 on the permeate side surface is also neglected. The jumping rate is defined as,

$$k_{i,j} = v_0 \exp(\frac{-E_{i,j}^a}{k_B T}), \qquad (1)$$

where the prefactor v_0 is estimated as $v_0 = k_B T/h = 4.2 \times 10^{10}$ T/Ks, $E_{i,j}^a$ is the activation energy for H jumping from site i to j, k_B is the Boltzmann constant, and T is the temperature. A sufficiently small uniform time step ($\Delta t << \frac{1}{k_{i,j}}$) is adopted for each jump. As the feed side surface is assumed to be always fully occupied by atomic H, hopping from subsurface to surface is forbidden ($k_{1,0} = 0.0$, denoting a high pressure limit), and the reverse process is allowed with a

10

rate $k_{0,1}$. Hydrogen concentration on each layer evolves from 0.0 to $c_i\,(t)\leqq 1.0$ with an increment rate of

$$\frac{\partial c_i(t)}{\partial t} = c_{i-1}(t)k_{i-1,i} + c_{i+1}(t)k_{i+1,i} - c_i(t)k_{i,i-1} - c_i(t)k_{i,i+1}. \qquad (2)$$

When $\int_{\tau}^{\tau+\Delta t}\Delta c_i(t)dt \rightarrow 0$, the ith layer is saturated with H. The decomposition, recombination, surface-subsurface, and subsurface-bulk diffusion barriers are from our DFT calculations of the 4Pd, 3Pd1Ag, and 3Pd1Cu films, even though our simulations include much thicker films than 4 ML total. We consider the layers inside the subsurface as bulk-like, and the corresponding H penetration barriers are calculated from H diffusion in bulk Pd.
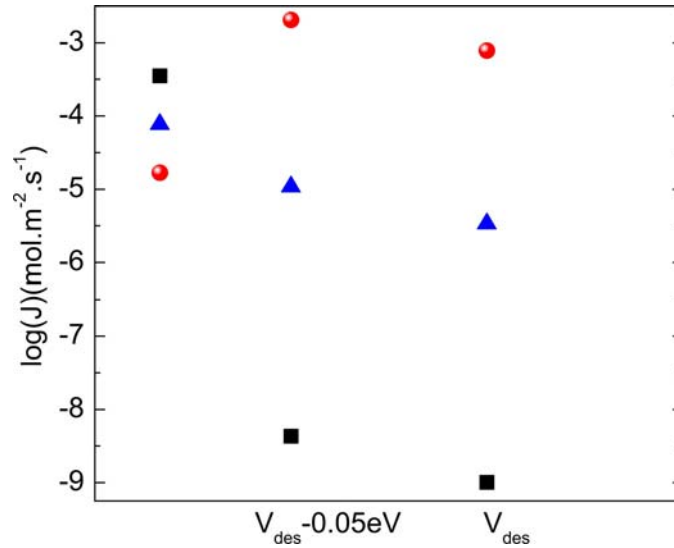

Figure 3. Logarithmic of H$_2$ flux through a 4-ML Pd film as a function of temperature. The H$_2$ desorption barrier adopted: right column, 1.36 eV, adopted from the surface of 4Pd; left column, 1.31 eV, as reduced by the upper limit (0.05eV) due to QSE.
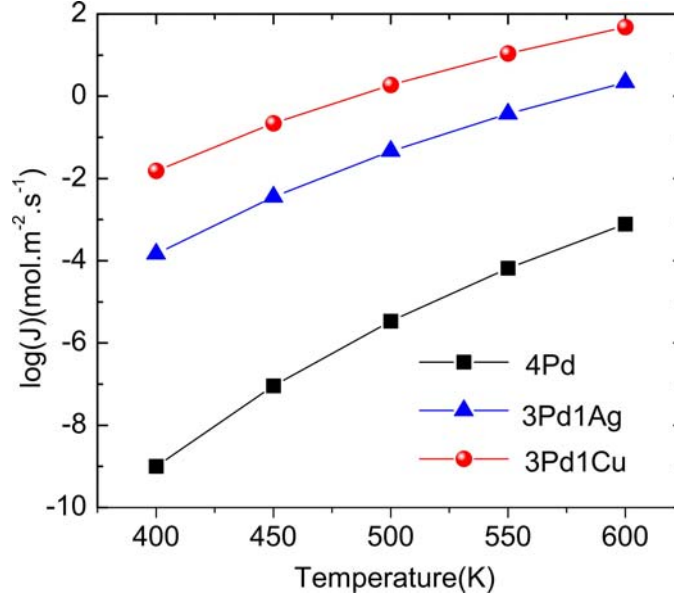
Figure 4. Logarithmic of the H_2 flux as a function of the temperature through the symmetric 4Pd and asymmetric 3Pd1Ag and 3Pd1Cu films.

E. H_2 permeance of the symmetric and asymmetric quantum Pd films

Equilibrium H_2 flux is very rapid to reach for all of the three systems if the total thickness is in the quantum regime. For example, even for 100-ML films, the time to get saturation is only on the order of 10^{-7} s at 600K. Therefore, we can ignore the influence of the transient behavior on the performance of the films. As expected, the steady state H_2 flux follows the Arrhenius relation $J = \theta v_0 \exp(\frac{-E_{des}^a}{k_B T})$, where θ is the concentration of the chemisorbed H dimers on the permeate side surface, and E_{des}^a is the associative desorption barrier. For a given type of films, the flux is determined only by the concentration of H dimers on the permeate side surface and the desorption rate. On one hand, since the surface H-reactivity of pure quantum Pd films varies by less than 0.05 eV induced by QSE, the H_2 flux can be tuned by only several times (Figure 3).

12

On the other hand, dramatic changes in the H_2 flux can be expected as we go from a pure Pd film to the functionalized Pd films. Moreover, for a given E_{des}^a, the variation of membrane thickness is small perturbations to J because surface effects rather than bulk diffusion determine the hydrogen flux. e.g., The quasi-steady state J is 7.82×10^{-4} and 7.81×10^{-4} for 10 and 100 ML, respectively ($\Delta J = 10^{-6}$ mol.m^{-2}.s^{-1}) at 600K. As can be seen from Figure 4, the H_2 flux in the temperature range of 400-600K through the asymmetric 3Pd1Ag and 3Pd1Cu films are about 3-5 and 5-7 orders of magnitude larger than that through the symmetric 4Pd film. These dramatic findings contradict qualitatively with the experimental observation that the permeability is reduced for the asymmetric Pd membranes coated with Cu films.[366] The contradiction is attributed to the endothermic nature of atomic H dissolution in bulk Cu and the corresponding lower solubility and diffusivity compared with that in bulk Pd.[20,34,35] The thinnest Cu coating layer used in the earlier experiments was 2.9 nm, much thicker than the single Cu coating layer suggested in the present study. In particular, our present study strongly indicates that dramatic flux enhancement is expected in future controlled experiments exploiting quantum (N-1)Pd1Cu and (N-1)Pd1Ag films.

We perform thermodynamic analysis to evaluate the influences of finite pressure and temperature and to justify the approximations made in our rate equation model. Within the ideal-gas law, the chemical potential of H, μ_H, is determined by[45]

$$\mu_H(T, p) = \mu_H(T, p^0) + \frac{1}{2} k_B T \ln(\frac{p}{p^0}), \qquad (3)$$

where the pressure $p^0 = 1$ atm, and $\mu_H(T, p^0)$ was taken from the NIST-JANAF thermodynamical tables.[46] The chemical potential for half of the free H_2 as a function of the pressure and temperature is plotted in Figure 5. The binding energies of H on the feed side subsurfaces of all the three systems are similar (about -0.34 eV, Figure 2). Hydrogen prefers to stay on the subsurface rather than in the free molecule phase below 550K at 1 atm (Figure 5). Thus, it is valid to neglect the subsurface-to-surface hopping of atomic H on the feed side, while keeping the surface saturated with H below this temperature. For 3Pd1Cu, when the permeate side is kept in a low pressure (10^{-5} atm) and the temperature is higher than 320K, the free H_2 state is favored over the H chemisorption state on the surface. For the case of 3Pd1Ag, hydrogen always prefers the free H_2 phase, rather than the binding state on the surface of Ag. However, for symmetric Pd films, higher vacuum conditions on the permeate side are needed to avoid the dissociative adsorption of permeated H_2. That is, with the pressure of 1 atm on the feed side and 10^{-5} atm on the permeate side, our approximation is valid in the temperature range of 320-550K for 3Pd1Cu and 0-550K for 3Pd1Ag; however, for the pure Pd film, a much higher vacuum on the permeate side is required. Moreover, as the chemical potential of free H_2 at finite temperature and pressure decreases (Figure 5), the H_2 desorption barriers will be reduced and the H_2 flux will thus be higher.[43,44] As yet another cross validity check in connection with existing studies, the hydrogen flux obtained by our numerical model is comparable with the experimental results of Chen et al. in the surface-effect dominated regime.[47] Moreover, our results are also quantitatively consistent with the results of other models[48] when the same hydrogen desorption barrier is adopted.
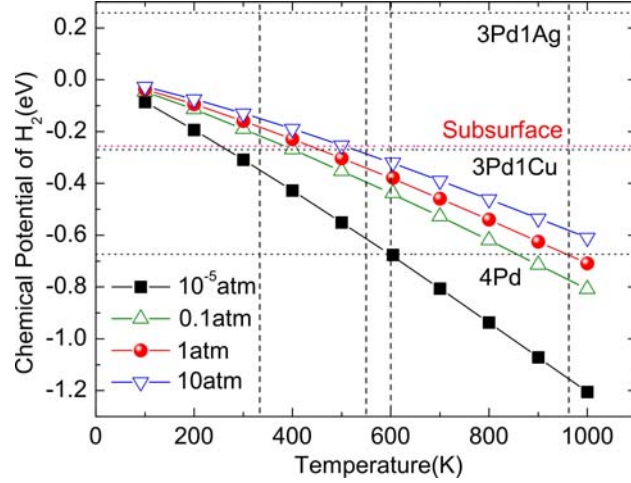
Figure 5. The chemical potential of free H_2 in the gas phase as a function of temperature and pressure. The horizontal black dotted lines indicate the H binding energy on the permeate side surface of 4Pd, 3Pd1Cu, and 3Pd1Ag, and the red dotted line indicates the H binding energy on the feed side subsurface; the vertical dashed lines are used to guide the eyes.

We next discuss the influences of H-H interaction on the magnitude of H_2 flux. If H-H interaction is taken into account, the hopping rate in the diffusion equation becomes dependent on the H concentration. From our DFT calculations, we find that H atoms on two adjacent *fcc* sites of the surface of 4Pd, 3Pd1Cu, and 3Pd1Ag are slightly repulsive (~0.02-0.05 eV), while the repulsive energy between the neighboring *hcp* and *fcc* is about 0.20 eV. The repulsive interaction between two closest H atoms at the octahedral interstitial sites within the permeate side subsurface of 3Pd1Ag is 0.01eV, while that at the octahedral-tetrahedral sites is 0.60 eV. Thus, H will hardly occupy the tetrahedral sites, consistent with previous results.[49] The hopping rate tends to decrease as the concentration of the diffusing particles increases if the inter-particle interaction is attractive, and it tends to increase for a repulsive inter-particle interaction.[43,44] Therefore, the atomic H hopping rates inside the films will be larger when the H-H interaction is considered, and the resulting H_2 flux will be further enhanced.

15

Despite the obvious advantages of thin palladium films for hydrogen permeation, issues exist limiting their applications, such as feed side contamination by molecular gas mixtures and high hydrogen concentration induced embrittlement.[50-52] One route to solve this problem is to use Pd-based metal alloys as membranes, which the current inorganic membrane technology community mainly focuses on.[53-55] In the quantum film community, the fabrication of atomically flat metal alloys in the quantum regime becomes feasible even for two metal elements immiscible in the bulk form,[5] and the amount of Pd consumed will be significantly reduced compared with the conventional thick membranes. Moreover, for applications of the coating systems in hydrogen purification, especially with high temperature annealing, one disadvantage is the intermixing of the coating element and the substrate at the interface.[23,33] However, even if interfacial alloy is formed in our asymmetric films, the rate-limiting barriers should shrink though compared with that of the pure palladium films considering the energetics and kinetics of H_2 penetrating through a metal film. Therefore, we expect that Pd_xCu_{1-x} alloy with thickness in the quantum regime can be used as hydrogen purification membrane with the ability to resist sulfur containing poisoning and simultaneously also to increase the hydrogen flux by reducing the rate-limiting barrier.

IV Conclusions

In summary, we have used a multi-scale approach combining first-principles calculations with rate equation simulations to explore how quantum size effects (QSEs) and QSE-based functionalization can alter the energetics and kinetics of H_2 transports through ultrathin Pd metal films. The quantum Pd films are found to possess extra (or magic) stability at certain film

thickness. The H_2 flux through such quantum films are demonstrated to be tuned dramatically by the QSE-induced variations in the key molecular/atomic rate processes. Most strikingly, coating the permeate side of the Pd quantum films with only one layer of less H-reactive Cu or Ag element can significantly reduce rate-limiting barrier of pure Pd and thus enhances the H_2 flux around 500 K by 5-7 or 3-5 orders of magnitude, respectively. These novel findings are fundamentally intriguing in their own right, and also point to new directions in materials discoveries for advanced hydrogen purification technologies.

*Email: jlwang@seu.edu.cn
† Email: wzhu3@utk.edu

REFERENCES

1. A. R. Smith, K. J. Chao, Q. Niu, and C. K. Shih, Science **273**, 226-228 (1996).

2. Z. Y. Zhang, Q. Niu, and C. K. Shih, Phys. Rev. Lett. **80**, 5381-5384 (1998).

3. J. J. Paggel, T. Miller, and T. C. Chiang, Science **283**, 1709-1711 (1999).

4. Y. Guo, Y. F. Zhang, X. Y. Bao, T. Z. Han, Z. Tang, L. X. Zhang, W. G. Zhu, E. G. Wang, Q. Niu, Z. Q. Qiu, J. F. Jia, Z. X. Zhao, and Q. K. Xue, Science **306**, 1915-1917 (2004).

5. M. M. Özer, Y. Jia, Z. Y. Zhang, J. R.Thompson, and H. H. Weitering, Sciecne **316**, 1594–1597 (2007).

6. S. Qin, J. Kim, Q. Niu, and C. K. Shih, Science **324**, 1314-1317 (2009).

7. C. M. Wei and M. Y. Chou, Phys. Rev. B **66**, 233408 (2002).

8. Y. Jia, B. Wu, H. H. Weitering, and Z. Y. Zhang, Phys. Rev. B **74**, 035433 (2006).

9. A. G. Danese, F. G. Curti, and R. A.Bartynski, Phys. Rev. B **70**, 165420 (2004).

10. L. Aballe, A. Barinov, A. Locatelli, S. Heun, and M. Kiskinova, Phys. Rev. Lett. **93**, 196103 (2004).

11. N. Binggeli and M. Altarelli, Phys. Rev. Lett. **96**, 036805 (2006).

12. V. S. Stepanyuk, N. N. Negulyaev, L. Niebergall, R. C. Longo, and P. Bruno, Phys. Rev. Lett. **97**, 186403 (2006).

13. X. C. Ma, P. Jiang, Y. Qi, J. F. Jia, Y. Yang, W. H. Duan, W. X. Li, X. H. Bao, S. B. Zhang, and Q. K. Xue, Proc. Natl. Acad. Sci. USA **104**, 9204–9208 (2007).

14. P. Jiang, X. C. Ma, Y. X. Ning, C. L. Song, X. Chen, J. F. Jia, and Q. K. Xue, J. Am. Chem. Soc. **130**, 7790-7791 (2008).

15. C. L. Song, Y. L. Wang, Y. X. Ning, J. F. Jia, X. Chen, B. Sun, P. Zhang, Q. K. Xue, X. C. Ma, J. Am. Chem. Soc. **132**, 1456-1457 (2010).

16. W. G. Zhu, H. Chen, K. H. Bevan, and Z. Y. Zhang, ACS Nano **5**, 3707–3713 (2011).

17. J. L. Qu, B. Sun, J. Zheng, R. Yang, Y. T. Wang, and X. G. Li, J. Power Sources **195**, 1190-1194 (2010).

18. T.-L. Chan, C. Z. Wang, M. Hupalo, M. C. Tringides, and K. M. Ho, Phys. Rev. Lett. **96**, 226102 (2006).

19. L. Y. Ma, L. Tang, Z. L. Guan, K. He, K. An, X. C. Ma, J. F. Jia, Q. K. Xue, Y. Han, S. Huang, and F. Liu, Phys. Rev. Lett. **97**, 266102 (2006).

20. A. J. De Rosset, Ind. Eng. Chem. **52**, 525– 528 (1960).

21. J. N. Armor, J. Membr. Sci. **147**, 217–233 (1998).

22. Uemiya, S. Sep. Purif. Methods **28**, 51-85 (1999).

23. N. W. Ockwig and T. M. Nenoff, Chem. Rev. **107**, 4078–4110 (2007).

24. K. R. Hwang, S. K. Ryi, C. B. Lee, S. W. Lee, and J. S. Park, Int. J. Hydrogen Energy **36**, 10136-10140 (2011).

25. C. Langhammer, I. Zorić, and B, Kasemo, Nano Lett. **7**, 3122-3127 (2007).

26. X. Q. Zeng, M. L. Latimer, Z. L. Xiao, S. Panugant, U. Welp, W. K. Kwok, and T. Xu, Nano Lett. **11**, 262-268 (2010).

27. P. Kamakoti, B. D. Morreale, M. V. Ciocco, B. H. Howard, R. P. Killmeyer, A. V. Cugini, and D. S. Sholl, Science **307**, 569–573 (2005).

28. D. S. Sholl and Y. H. Ma, RS Bulletin **31**, 770-773 (2006).

29. Y. Zhang, M. Komaki, and C. Nishimura, J. Membr. Sci. **246**, 173–180 (2005).

30. Ø. Hatlevik, S. K. Gade, M. K. Keeling, P. M. Thoen, A. P. Davidson, and J. D. Way, Sep. Purif. Technol. **73**, 59–64 (2010).

31. S. H. Israni and M. P. Harold, Ind. Eng. Chem. Res. **49**, 10242–10250 (2010).

32. S. Q. Huang, S. H. Tang, X. L. Mu, Y. Dai, G. X. Chen, Z. Y. Zhou, F. X. Ruan, Z. L. Yang, and N. F. Zheng, Nat. Nanotechnol. **6**, 28–32 (2011).

33. C. –J. Chung, S. C. Lee, J. R. Groves, E. N. Brower, R. Sinclair, and B. M. Clemens, Phys. Rev. Lett. **108**, 106102 (2012).

34. P. B. Lloyd, J. W. Kress, and B. J. Tatarchuk, Appl. Surf. Sci. **119**, 275–287 (1997).

35. S. Kandoi, P. A. Ferrin, and M. Mavrikakis, Top. Catal. **53**, 384–392 (2010).

36. P. L. Andrew and A. A Haasz, J. Appl. Phys. **70**, 3600–3604 (1991).

37. G. Kresse and J. Furthmüller, Phys. Rev. B **54**, 11169-11185 (1996).

38. J. P. Perdew, K. Burke, and M. Ernzerhof, Phys. Rev. Lett. **77**, 3865-3868 (1996).

39. G. Henkelman, B. P. Uberuaga, and H. Jónsson, J. Chem. Phys. **113**, 9901–9904 (2000).

40. M. Wilde and K. Fukutani, Phys. Rev. B **78**, 115411 (2008).

41. B. Hammer and J. K. Nøskov, Surf. Sci. **343**, 211–220 (1995).

42. N. Ìnoglu and J. R. Kitchin, Mol. Simulat. **36**, 633–638 (2010).

43. *Diffusion in Condensed Matter: Methods, Materials, Models*, Heitjans, P.; Kärger, J., Eds.; Springer: Berlin, 2005.

44. *The Metal-Hydrogen System*, Fukai, Y., Eds.; Springer: Berlin, 2005.

45. K. Reuter and M. Scheffler, Phys. Rev. B **65**, 035406 (2001).

46. M. W. Jr. Chase, in 1998 *NIST-JANAF thermochemical tables*, 4th Ed., American Institute of Physics: New York.

47. W. H. Chen, P. C. Hsu, B. J. Lin, Int. J. Hydrogen Energ. **35**, 5410-5418 (2010).

48. T. L. Ward and T. Dao, J. Membr. Sci. **153**, 211–231 (1999).

49. T. B. Flanagan and W. A. Oates, Annu. Rev. Mater. Sci. **21**, 269–304 (1991).

50. F. Roa, M. J. Block, and J. D. Way, Desalination **147**, 411-416 (2002).

51. F. Scura, G. Barbieri, G. De Luca, and E. Drioli, Int. J. Hydrogen Energ. **33**, 4183–4192 (2008).

52. C. H. Chen and Y. H. Ma, J. Membr. Sci. **362**, 535–544 (2010).

53. P. Kamakoti and D. S. Sholl, J. Membr. Sci. **279**, 94-99 (2006).

54. L. Semidey-Flecha and D. S. Sholl, J. Chem. Phys. **128**, 144701 (2008).

55. S. G. Kang, K. E. Coulter, S. K. Gade, J. D. Way, and D. S. Sholl, J. Phys. Chem. Lett. **2**, 3040–3044 (2011).